2-(4′,4′-Dimethyl-3′,4′-dihydrooxazol-2′-yl)phenol: Some First-Row Transition Metal Complexes of This Naturally Occurring Binding Group

Govindasamy Mugesh,[a] Harkesh B. Singh,*[a] and Ray J. Butcher[b]

Dedicated to Prof. B. L. Khandelwal on the occasion of his 63rd birthday

Keywords: Oxazolines / Metal assisted hydrolysis / Hydrogen bonds / Chirality / Siderophores

The synthesis and characterization of monomeric Mn^{III}, Co^{II}, Ni^{II}, Cu^{II}, and Zn^{II} phenolates derived from a biologically relevant ligand, 2-(4′,4′-dimethyl-3′,4′-dihydrooxazol-2′-yl)-phenol (**1**), are described. The addition of $Mn(OAc)_2 \cdot 4\,H_2O$ to an ethanolic solution of **1** affords an unexpected 1:3 complex $[Mn(OR)\{O(Ox)\}_2]$ (**2**) [R = $C_6H_4CONHC(Me_2)CH_2OH$, Ox = 2-(4,4-dimethyl-2-oxazolinyl)phenyl] in which one of the five-membered oxazoline rings is partially hydrolyzed. The complexes $[M\{O(Ox)\}_2]$ [M = Co (**3**), Ni (**4**), Cu (**6**), or Zn (**7**)] were prepared in good yield by the reactions of **1** with the corresponding metal acetates. Novel formation of the six-coordinate Ni^{II} complex **5** with neutral acetic acid was observed during the crystallization process. The complexes were characterized by elemental analysis, magnetic susceptibility, as well as EPR, ^1H NMR, electronic, and mass spectral techniques. Complexes **2**, **3**, **5**, **6**, and **7** were characterized by single crystal X-ray diffraction studies. Complex **2** is six-coordinate whereas complexes **3**, **6**, and **7** are four-coordinate with two oxazoline bidentate ligands. The geometry around the metal center is found to be distorted tetrahedral for all of the four-coordinate complexes. Complex **5** is octahedral with four coordination sites occupied by the two bidentate oxazoline ligands and the other two are occupied by two neutral acetic acid molecules. The hydroxy groups of the coordinated acetic acid are hydrogen-bonded to the phenolate oxygen atoms of the oxazoline ligands. The variable-temperature ^1H NMR spectroscopic studies of complex **7** indicate that the interconversion between the (*M*) and (*P*) helix is slow at low temperatures.

Introduction

Interest in the biochemistry of 2-(2-hydroxyphenyl)-2-oxazoline started with the finding that this ligating moiety is present as a naturally occurring iron chelator in some classes of siderophores such as mycobactine, parabactin, and vibriobactin.[1]

Owing to the strong chelating ability of the oxazoline ligand and its high affinity for Fe^{III}, the siderophores have been shown to be highly potent in the deferration of mammalian cell lines and are potentially useful for chelation therapy.[2] The use of oxazoline ligands in a wide range of catalytic reactions has also been reported in recent years.[3] In this regard much effort has been directed towards the synthesis and catalytic applications of metal complexes containing 2-(2′-hydroxyphenyl)-2-oxazoline ligands.[4] Recently, Ti^{IV} and Zr^{IV} complexes of 2-(2′-hydroxyphenyl)-2-oxazolines have been used for some homogeneous catalytic reactions such as Mukaiyama reaction, allylations, hydrocyanations, Diels–Alder reactions.[4b] In these cases, the bis-(oxazoline)-ligated transition metal Lewis acids displayed activity for almost all commonly encountered Lewis acid promoted reactions. More recently, Ni^{II}, Pd^{II}, and Mn^{III} complexes of chiral oxazoline ligands containing N,O and N,P moieties and Mn^{III} complex of 2-(2′-hydroxyphenyl)-2-oxazoline have been used for the catalytic epoxidation of styrene.[5]

Although a few complexes of 2-(2′-hydroxyphenyl)-2-oxazolines with trivalent and divalent metal ions are known,[6–8] very little information is available about their structural chemistry. As part of our work on intramolecularly coordinated organochalcogens,[9] we have recently described the synthesis and characterization of Group 12 metal chalcogenolates (S, Se, Te) with bidentate oxazoline ligands.[10] Interestingly, the (thiolato)-[10a] and (selenolato)-zinc[10b] complexes were found to be chiral at room temperature and interconversion between the (*M*) and (*P*) helix was slow at room temperature. Replacement of the S or Se by Te led to the faster interconversion between the (*M*) and (*P*) forms. A similar trend was observed when the central metal ion was varied. It was observed that the interconversion of enantiomers at small metal ions, such as zinc, was slower whereas at the larger metal ions, such as mercury, it was much faster even at low temperature. Since the isolation of "helically" chiral metal complexes of zinc with lighter chalcogens (S, Se) was found to be more facile than the complexes with the heavier chalcogen (Te), it was thought worthwhile to extend our approach to the lightest chalcogen (oxygen) as well. Also, in order to generalize our observations, we extended our approach to other transition metals where the isolation of the tetrahedral complexes was

[a] Department of Chemistry, Indian Institute of Technology
Powai, Bombay 400076, India
Fax: (internat.) + 91-22/572-3480
E-mail: chhbsia@chem.iitb.ernet.in
[b] Department of Chemistry, Howard University
Washington, DC 20059, USA

  1434–1948/01/0303–0669 $ 17.50+.50/0

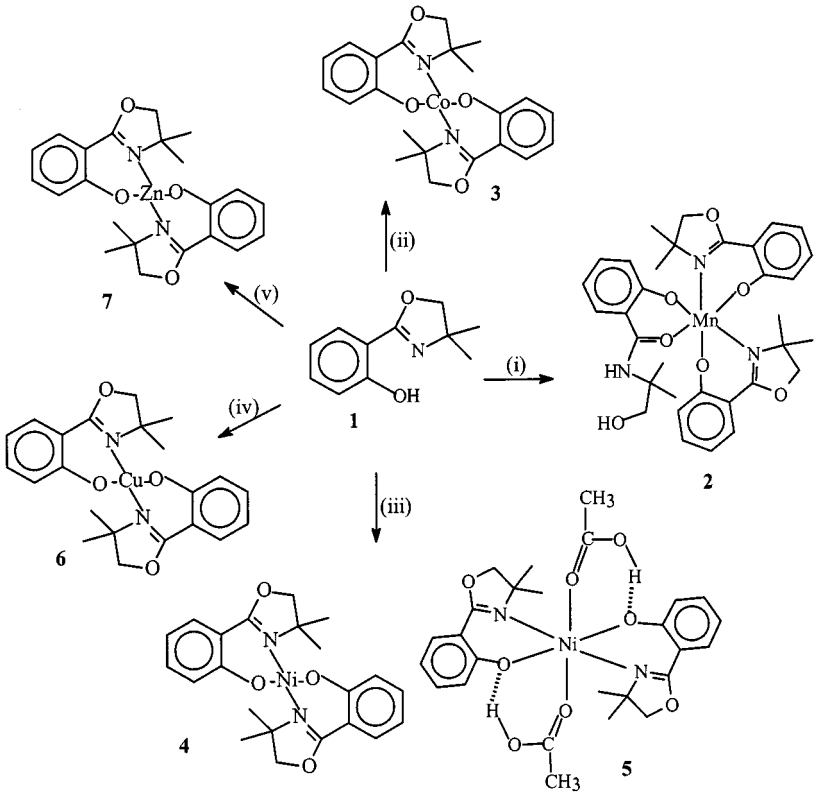

Scheme 1. Synthetic route to the metal complexes **2**–**7**; reagents and conditions: i) $Mn(OAc)_2 \cdot 4\,H_2O$, EtOH, room temp., 24 h; ii) $Co(OAc)_2 \cdot 4\,H_2O$, EtOH, room temp., 12 h; iii) $Ni(OAc)_2 \cdot 4\,H_2O$, EtOH, room temp., 18 h; iv) $Cu(OAc)_2 \cdot H_2O$, EtOH, room temp., 24 h; v) $Zn(OAc)_2$, EtOH, room temp. 24 h

feasible. In this paper we describe the synthesis and characterization of Mn^{III}, Co^{II}, Ni^{II}, Cu^{II}, and Zn^{II} complexes with the naturally occurring 2-(2′-hydroxyphenyl)-2-oxazoline ligating moiety.

Results and Discussion

Synthesis

The ligand 2-(4′,4′-dimethyl-3′,4′-dihydrooxazol-2′-yl)-phenol (**1**) was prepared in a one-pot synthesis by following the published procedure with minor modifications.[5] Since the proton of the hydroxy group in the oxazoline was acidic enough to react with the metal salts containing basic anion acetate, the ligand was treated with various metal acetates in absolute ethanol to obtain the corresponding metal complexes (Scheme 1). The addition of $Mn(OAc)_2 \cdot 4\,H_2O$ to an ethanolic solution of **1** afforded a black-green solution of complex **2**. Elemental analysis of the black-green crystals obtained upon slow evaporation of the solvent did not match with the expected 1:2 complex. Instead, it indicated the formation of a 1:3 complex where manganese was in a +3 oxidation state. Interestingly, one of the oxazoline rings undergoes a metal-assisted hydrolysis (vide infra) in the presence of acetic acid produced during the reaction. However, no hydrolysis of the oxazoline ring was observed with the other metal ions.

The partial hydrolysis of the oxazoline ring in complex **2** is similar to the hydrolysis of the active site of Agrobactin, a siderophore from *Agrobacterium tumefaciens*. The oxazoline ring of the siderophore hydrolyzes in the presence of an acid to give the open-chain form, Agrobactin A (Scheme 2).[1a] It has been further reported by Neilands et al. that the replacement of the −OH group in the 2-position of the benzene ring with −OMe or −OBz groups in Agrobactin led to a facile opening of the oxazoline ring.[1c] Similarly, in ligand **1** the coordination of the nitrogen atom to the metal center probably disturbs the co-planarity of the oxazoline ring leading to hydrolysis of the five-membered ring in the presence of acetic acid. The partial hydrolysis of the oxazoline ring is also noteworthy since acid hydrolysis of the oxazoline ring in complex **2** leads to the formation of an amide instead of the expected acid (−COOH). The mechanism of the hydrolysis involves the formation of the oxazolium ion. The oxazolium ion so formed presumably then

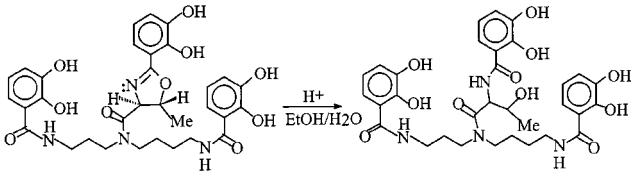

Scheme 2. Acid-catalyzed hydrolysis of the oxazoline ring present in the active site of Acrobactin to the open-chain from, Agrobactin A

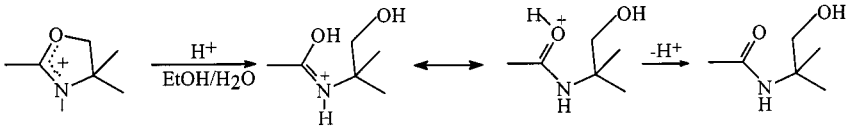

Scheme 3. Proposed mechanism of the hydrolysis of oxazoline ring in complex **2**

opens to afford the cleaved product which then undergoes tautomerization to give the open-chain amide (Scheme 3).[1a]

In order to determine whether the presence of air plays an important role in the ligand hydrolysis, the synthesis of complex **2** was attempted under nitrogen. In this case, a very air-sensitive green-colored gummy solid, presumably the expected Mn^{II} complex, was obtained. All efforts to obtain crystals of the Mn^{II} complex were unsuccessful. Isolation of the Mn^{III} complex under aerobic conditions further demonstrates that both the stability of the Mn^{III} oxidation state and its oxophilicity promote the ligand hydrolysis.

The addition of $Co(OAc)_2 \cdot 4\,H_2O$ to an ethanolic solution of **1** resulted in an immediate formation of Co^{II} complex **3** as a pink-colored solid. The crystals of the complex were obtained from a CH_2Cl_2/methanol (1:1) solution. When an ethanolic solution of **1** was added to a solution of $Ni(OAc)_2 \cdot 4\,H_2O$, an immediate formation of a green precipitate was observed. After 12 h of stirring at room temperature, the pale green solid obtained was filtered and washed with ethanol. Interestingly, the slow concentration of the filtrate afforded dark green crystals which were different from the compound obtained by filtration of the reaction mixture. Elemental analyses of both the products indicated that the pale green solid was the expected 1:2 complex **4** whereas the dark green crystalline solid (**5**) obtained from the filtrate was an acetic acid [produced in the reaction mixture during the reaction of $Ni(OAc)_2 \cdot 4\,H_2O$ with **1**] adduct of **4** (vide infra). The addition of acetic acid to an ethanolic solution of complex **4** also afforded complex **5**. Although four-coordinate Ni^{II} complexes are known to coordinate extra ligands in solution to set up equilibria between four-, five-, and six-coordinate complexes,[11] the strong bonding of the acetic acid molecules in this case is surprising since the recrystallization from methanol did not lead to the expected exchange.[11b] The Cu^{II} and Zn^{II} complexes **6** and **7** were prepared in good yields by the reaction of **1** with the corresponding metal acetates. All the complexes are quite soluble in common organic solvents such as CH_2Cl_2, $CHCl_3$, benzene, etc.

NMR Spectroscopy

Complex **7** was studied in solution by NMR spectroscopy. The ^1H NMR spectrum of **7** in $CDCl_3$ showed only small chemical shift differences compared with the spectrum of **1**. We have recently observed an AB spin behavior of the methylene protons in the corresponding zinc thiolate and selenolate complexes, and used it as a diagnostic probe for their chirality.[10a,10b] For complex **7**, no such behavior was observed at room temperature and the signals for the methyl and methylene protons were observed as singlets. However, the signals due to the methyl and methylene protons were slightly broad and this showed that the complex was probably not rigid at room temperature. At −55 °C, the $-CH_3$ protons gave rise to two singlets and the $-CH_2-$ protons gave an AB quadruplet (Figure 1). When the solution was heated to 50 °C, the two signals observed for the methyl protons and the AB quadruplet for the methylene protons became sharp singlets. This clearly indicates that the interconversion of the (*M*) and (*P*) helix is fast at room temperature and becomes slow at a low temperature on the NMR spectoscopic time scale. A similar behavior was observed at low temperatures for the cadmium thiolate, selenolate, and tellurolate complexes derived from 4,4-dimethyl-2-phenyloxazoline.[10] The ^{13}C NMR spectrum of **7** was re-

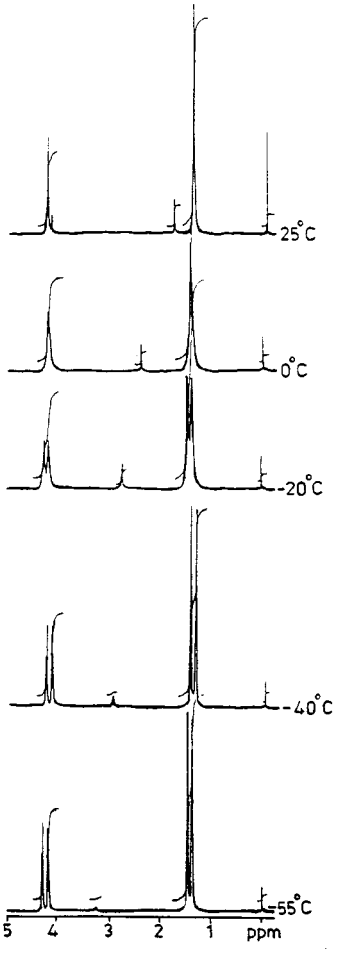

Figure 1. Variable-temperature ^1H NMR ($CDCl_3$, 300 MHz) spectra (in part only) of **7** at −55°C, the signals due to the $-CH_2-$ and $-CH_3$ protons split into an AB quadruplet and two singlets, respectively

corded in $CDCl_3$. The methyl and methylene carbon signal were shifted upfield with respect to those of **1**. The signals for the oxygen-bearing aromatic carbon atom and C(2) of the heterocycle were significantly shifted downfield (δ = 160.2 and 165.3 for **1**, δ = 170.0 and 170.5 for **7**).

Magnetic Properties

The room-temperature magnetic moment of the black-green manganese(III) complex **2** is 3.33 BM which indicates that the complex is low-spin (S = 1). The observed magnetic moment of **2** is considerably larger than the spin-only value of 2.83 BM for two unpaired electrons. This result is attributable to the presence of the orbital angular momentum for the ground term ion. Mn^{III} is known to form low-spin octahedral complexes only with strong donors like cyanides, oximes, or porphyrins. Complex **2** provides a rare example of a low-spin Mn^{III} complex with N and O donors from the oxazoline ligand. Although the effective magnetic moments for the tetrahedral Co^{II} complexes are normally observed close to the spin-only values, the observed magnetic moment for the Co^{II} complex **3** (μ_{eff} = 4.57 BM) is much higher than the spin-only magnetic moment (μ = 3.87 BM) for three unpaired electrons. This discrepancy may again be caused by angular momentum introduced to the ground state (A_2) by mixing of higher T states. The magnetic moment of 3.05 BM determined for the octahedral Ni^{II} complex **5** is very close to the spin-only value for two unpaired electrons, whereas the magnetic moment observed for tetrahedral Ni^{II} complex **4** (3.42 BM) is much higher than the spin-only value. This is in agreement with the general observation that octahedral Ni^{II} complexes have less orbital momentum than the tetrahedral complexes. It is known that the magnetic moment of truly tetrahedral Ni^{II} complexes should be about 4.2 BM because of the ground state, $^3T_1(F)$, which has much inherent orbital angular momentum. However, it is also reported that even slight distortion in the geometry reduces this markedly by splitting the orbital degeneracy. Thus, fairly regular tetrahedral complexes have moments of 3.5−4.0 BM, while for the more distorted ones the moments are 3.0−3.5 BM, i.e. in the same range as for six-coordinate complexes. The magnetic moment observed for **4**, therefore, suggests that the geometry around the metal ion is highly distorted. The magnetic moment of complex **6** (1.76 BM) is very close to the spin only value (1.73 BM) for one unpaired electron. The geometry around the metal center is, therefore, predicated as planar since a higher orbital contribution to the magnetic moment is expected for a tetrahedral Cu^{II} complex than for a planar one.[12]

Electronic Spectra

The solution-phase electronic spectrum (> 200 nm) of the ligand **1** consists of two relatively intense bands centered at 255 nm (ε_{max} = 47500 $M^{-1}cm^{-1}$) and 303 (ε_{max} = 36600 $M^{-1}cm^{-1}$), involving $\pi\rightarrow\pi^*$ transitions, and a low-intensity feature (ε_{max} = 2500 $M^{-1}cm^{-1}$) in the 350−360 nm region, responsible for the yellow color, and presumably involving $n\rightarrow\pi^*$ excitation. The electronic spectrum of **2** is dominated by a peak with medium intensity centering at 303 nm (ε_{max} = 7480 $M^{-1}cm^{-1}$), attributable to the $\sigma(N)\rightarrow Mn^{III}$ ligand-to-metal charge-transfer (LMCT) transition. One broad band at 658 nm (ε_{max} = 191 $M^{-1}cm^{-1}$) may be attributed to the ligand field transition. A broad peak centered at 500 nm (ε_{max} = 357 $M^{-1}cm^{-1}$) is also attributed to d-d transition. Four-coordinate tetrahedral and pseudo-tetrahedral Co^{II} complexes are commonly intense blue or green in color. Complex **3** shows pink color in the solid state as well as in solution. However, this is not surprising since a few complexes with dipivaloylmethane are known to give a pink color in solution.[13,14] In the tetrahedral Co^{II} case, there are three regions of absorption and, therefore, three spin-allowed electronic transitions are expected. Three d-d transition bands were observed as weak features at 501 nm (ε_{max} = 110 $M^{-1}cm^{-1}$), 563 (ε_{max} = 90 $M^{-1}cm^{-1}$), and 619 (ε_{max} = 30 $M^{-1}cm^{-1}$). The splitting of the middle band is probably due to spin-orbit coupling. There are four strong absorption bands in the high-energy region, 244 nm (ε_{max} = 33850 $M^{-1}cm^{-1}$), 281 nm (ε_{max} = 12070 $M^{-1}cm^{-1}$), 312 nm (ε_{max} = 10000 $M^{-1}cm^{-1}$), and 344 nm (ε_{max} = 11750 $M^{-1}cm^{-1}$), which can be assigned to the ligand transitions and charge-transfer transitions. For **4**, two bands, observed at 689 nm (ε_{max} = 15 $M^{-1}cm^{-1}$) and 591 nm (ε_{max} = 12 $M^{-1}cm^{-1}$), can be attributed to d-d transitions. There are three strong absorption bands in the high-energy region, 246 nm (ε_{max} = 12900 $M^{-1}cm^{-1}$), 309 nm (ε_{max} = 4730 $M^{-1}cm^{-1}$), and 336 nm (ε_{max} = 2590 $M^{-1}cm^{-1}$), which may be assigned to charge transfer and intra-ligand transitions. For **5**, there are two intense bands in the region between 200 and 340 nm that may be assigned to the intra-ligand $\pi\rightarrow\pi^*$ transitions. The band at 340 nm (ε_{max} = 1500 $M^{-1}cm^{-1}$) with medium intensity indicates the charge-transfer (CT) character. Finally, a weak feature (ε_{max} = 12 $M^{-1}cm^{-1}$) assigned to d-d transition, is present in the 500−600 nm range. For the Cu^{II} complex **6**, the ligand field transition occurs as a single broad band centering at 653 nm with an ε_{max} of 105 $M^{-1}cm^{-1}$. In addition two intense bands appear at higher energies. The peak that appears at 244 nm (ε_{max} = 30600 $M^{-1}cm^{-1}$) is assigned to the $\sigma(N)\rightarrow Cu^{II}$ LMCT transition.[15−17] The peak with medium intensity at 343 nm (ε_{max} = 11600 $M^{-1}cm^{-1}$) is too low for a charge-transfer transition involving an N donor. For tetrahedral Cu^{II} complexes with phenolate coordination, the $Cu^{II}\rightarrow$phenolate MLCT absorption occurs near 300 nm.[18,19] Therefore, the band at 309 nm (ε_{max} = 10600 $M^{-1}cm^{-1}$) is assigned as the higher energy $Cu^{II}\rightarrow\pi^*$-phenolate transition.

Electrochemistry

The cyclic voltammograms of **2−6** were recorded at room temperature in acetonitrile in the potential range −1.5 to +2.0 V vs. Ag/AgCl reference electrode. Complex **2** exhibits a quasi-reversible one-electron oxidation-reduction corresponding to the Mn^{IV}/Mn^{III} redox process ($E_{1/2}$ = 1.59 V; ΔE_p = 130 mV vs. Fc/Fc^+, $E_{1/2}$ = 0.38 V; ΔE_p = 100 mV at scan rate 50 mVs^{-1}). The Mn^{III}/Mn^{II} couple was not

observed up to −2.2 V, showing high stability of the Mn^{III} state in the present environment. Other complexes do not show any well-defined response in this potential range.

X-ray Crystallography

Crystal Structure of 2

Complex **2** crystallizes in the triclinic space group $P\bar{1}$. As can be seen in Figure 2, one of the five-membered oxazoline rings is partially hydrolyzed to give the open-chain form. The Mn^{III} ion present in the complex is six-coordinate where two nitrogen donor atoms of oxazoline rings and one carbonyl oxygen atom of the hydrolyzed oxazoline are coordinated to the central metal ion in addition to the aryloxo groups. Selected bond lengths and angles are summarized in Table 1. The three Mn−O−(Ar) bond lengths are close to each other but differ significantly from the distance between Mn and the carbonyl oxygen atom. The Mn−O and Mn−N bond lengths are comparable with the corresponding bond lengths reported for other related Mn^{III} pseudo-octahedral complexes.[19] The bond lengths and angles for the oxazoline ring reflect many similarities with the Agrobactin (Table 2).[1c] The intramolecular hydrogen bonds which are very similar to the ones observed in Agrobactin efficiently stabilize the molecular structure in the crystalline state. There are several weak interactions between the atoms in the crystal structure. Of these interactions, the hydrogen bonding between the NH proton and oxygen atom of the hydrolyzed oxazoline ring [O(33)···H−N(3) 2.266(6) Å; O(33)···N(3) 2.697(4) Å] is found to be much stronger than the others.

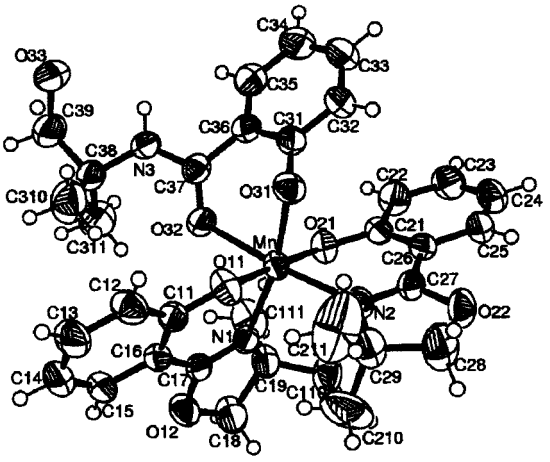

Figure 2. Crystal structure of complex **2**

Table 1. Selected bond lengths [Å] and angles [°] for **2**

Mn−N(1)	2.086(2)	Mn−N(2)	2.250(3)
Mn−O(21)	1.870(2)	Mn−O(11)	1.879(2)
Mn−O(31)	1.931(2)	Mn−O(32)	2.223(2)
O(21)−Mn−O(11)	178.39(10)	O(21)−Mn−O(31)	92.12(10)
O(11)−Mn−O(31)	88.86(10)	O(21)−Mn−N(1)	91.69(10)
O(11)−Mn−N(1)	87.60(9)	O(31)−Mn−N(1)	168.16(9)
O(21)−Mn−O(32)	91.71(9)	O(11)−Mn−O(32)	89.66(10)
O(31)−Mn−O(32)	84.07(9)	N(1)−Mn−O(32)	84.62(9)
O(21)−Mn−N(2)	86.11(9)	O(11)−Mn−N(2)	92.59(10)
O(31)−Mn−N(2)	91.49(10)	N(1)−Mn−N(2)	99.95(10)
O(32)−Mn−N(2)	174.99(9)		

Crystal Structure of 3

A perspective view of the molecule with an atom numbering scheme is shown in Figure 3. Compound **3** crystallizes as a neutral monomer in the $P\bar{1}$ space group of a triclinic system. The geometry around the Co^{II} center is tetrahedral with two bidentate oxazoline ligands. Selected bond lengths and angles are given in Table 3. The average Co−O bond length 1.9052 Å is significantly shorter than those reported for $Co(OAc)_2(imid)_2$ [1.984(1) Å][20] and $Co(OAc)_2$(2-Me-imid)$_2$ [2.098(1) Å].[21] The average Co−N bond lengths 1.9885 Å is also shorter than those observed for $Co(OAc)_2(imid)_2$ [2.0135(1) Å] $Co(OAc)_2$(2-Me-imid)$_2$ [2.062(3) Å]. The average chelate bite angle of O−Co−N is 94.57°. The larger bite angle leads to relatively smaller O−Co−O and N−Co−N angles of 119.23(7)° and 121.25(7)°, respectively. The O−Co−O angle of 119.23(7)° is higher than the corresponding value reported for Co-

Table 2. The bond lengths and angles for the oxazoline ring of complex **2** compared with those of the active site of Agrobactin

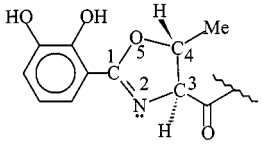

Agrobactin[a]		Complex **2**			
C(1)−N(2)	1.286(5)	N(1)−C(17)	1.288(4)	N(2)−C(27)	1.286(4)
C(3)−N(2)	1.464(5)	N(1)−C(19)	1.503(4)	N(2)−C(29)	1.485(4)
C(1)−O(5)	1.327(5)	O(12)−C(17)	1.353(3)	O(22)−C(27)	1.365(3)
C(4)−O(5)	1.466(5)	O(12)−C(18)	1.442(4)	O(22)−C(28)	1.428(4)
C(3)−C(4)	1.547(5)	C(18)−C(19)	1.526(5)	C(28)−C(29)	1.519(5)
C(1)−O(5)−C(4)	106.6(3)	C(17)−O(12)−C(18)	106.2(2)	C(27)−O(22)−C(28)	106.0(3)
C(1)−N(2)−C(3)	106.6(3)	C(17)−N(1)−C(19)	107.6(2)	C(27)−N(2)−C(29)	108.2(3)
O(5)−C(1)−N(2)	118.9(3)	O(12)−C(17)−N(1)	116.3(3)	O(22)−C(27)−N(2)	116.4(3)

[a] The atom numbering scheme of the active site of Agrobactin.

$(OAc)_2(2\text{-Me-imid})_2$ [105.1(1)°]. The interplanar angle between Co−O(11)−N(1) and Co−O(21)−N(2) is 94.7°.

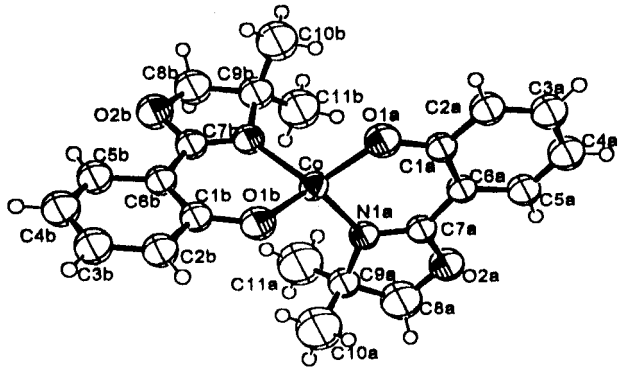

Figure 3. Crystal structure of complex **3**

Table 3. Selected bond lengths [Å] and angles [°] for **3**, **6**, and **7**

Bond lengths/angles	**3** M = Co	**6** M = Cu	**7** M = Zn
M−N(1)	1.9770(16)	1.985(1)	1.9866(19)
M−N(2)	1.9799(16)	1.986(2)	1.992(2)
M−O(11)	1.9025(15)	1.885(2)	1.9026(18)
M−O(21)	1.9075(14)	1.880(2)	1.9187(18)
O(11)−C(11)	1.312(2)	1.308(3)	1.308(3)
(12)−C(17)	1.349(2)	1.353(3)	1.356(3)
O(12)−C(18)	1.442(3)	1.439(3)	1.445(4)
O(21)−C(21)	1.309(2)	1.309(3)	1.302(3)
O(22)−C(27)	1.355(2)	1.347(3)	1.353(3)
O(22)−C(28)	1.451(3)	1.424(4)	1.448(4)
N(1)−C(17)	1.295(2)	1.298(3)	1.287(3)
N(1)−C(19)	1.494(2)	1.509(3)	1.488(3)
N(2)−C(27)	1.288(2)	1.297(3)	1.286(3)
N(2)−C(29)	1.497(2)	1.501(3)	1.497(3)
O(11)−M−O(21)	119.23(7)	156.04(9)	117.73(9)
N(1)−M−N(2)	121.25(7)	160.20(8)	121.14(9)
N(1)−M−O(21)	116.61(6)	92.05(7)	116.75(8)
N(2)−M−O(21)	94.03(6)	91.99(7)	94.16(8)
O(11)−M−N(1)	95.13(6)	91.76(7)	95.90(8)
O(11)−M−N(2)	112.52(7)	92.38(8)	112.90(9)

Crystal Structure of 5

The molecular structure of complex **5** is shown in Figure 4. Selected bond lengths and angles are presented in Table 4. The unit cell of **5** contains two nonsymmetric equivalent molecules. No significant differences between these two molecules are observed. The structure of complex **5** is found to be quite interesting. The Ni atom is six-coordinate and the geometry around the metal center is distorted octahedral. The Ni ion is bonded to two nitrogen and two oxygen atoms [both pairs are in the *cis* position (O−Ni−N angles 88.22−98.37°)] as well as two oxygen atoms of neutral acetic acid molecules. Interestingly, the acidic protons form strong hydrogen bonds with the aryloxo function of the ligand. This observation is similar to the one reported for a binuclear nickel(II) complex in which the neutral acidic acid molecule is involved in a hydrogen bonding with the alkoxo function.[11b] The C−O bond lengths of the coordinated oxygen atoms [C(12a)−O(3a) 1.223(3) Å, C(12b)−O(3b) 1.223(3) Å] are quite short while the distance of the noncoordinated oxygen atoms [C(12a)−O(4a) 1.302(4) Å, C(12b)−O(4b) 1.298(3) Å] are rather long. The bonding situation of the acetic acid molecules then allows for assuming double-bond-coordinated carbonyl groups C(12a)−O(3a) and C(12b)−O(3b) and C−O single bonds C(12a)−O(4a) and C(12b)−O(4b). The molecule has eight rings: two phenyl groups, two oxazoline groups, and four six-membered chelate rings; the latter are connected by the metal atom. The Ni(1)−N(1a) [2.075(2) Å] and Ni(1)−N(1b) [2.074(2) Å] distances are larger than those reported for four-coordinate Ni^{II} complexes with similar oxazoline ligands.[6] From the bond angle values it is observed that the two nitrogen atoms of the oxazoline five-membered rings and the two oxygen atoms of neutral acetic acid molecules form a square planar arrangement and the two phenolate oxygen atoms lie above and below the plane. The O(1a)−Ni(1)−O(1b) bond angle of 169.98(7)° indicates that these two atoms lie in the axial positions. The geometrical isomer isolated is, therefore, defined as the *cis* isomer.

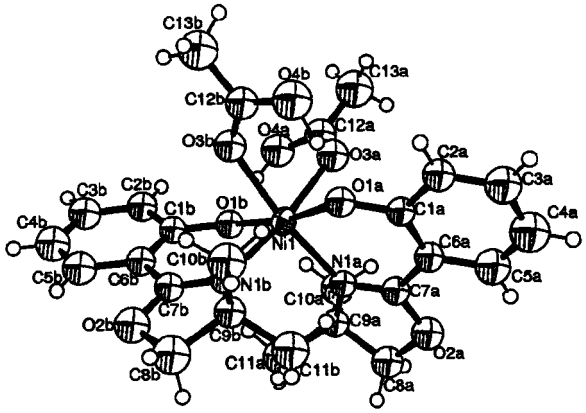

Figure 4. Crystal structure of complex **5**

Table 4. Significant bond lengths [Å] and angles [°] for **5**

Ni(1)−O(1a)	1.998(2)	Ni(1)−O(1b)	2.016(2)
Ni(1)−N(1b)	2.074(2)	Ni(1)−N(1a)	2.075(2)
Ni(1)−O(3b)	2.137(2)	Ni(1)−O(3a)	2.176(2)
O(1a)−Ni(1)−O(1b)	169.98(7)	O(1a)−Ni(1)−N(1b)	97.94(8)
O(1b)−Ni(1)−N(1b)	88.22(8)	O(1a)−Ni(1)−N(1a)	88.57(7)
O(1b)−Ni(1)−N(1a)	98.37(7)	N(1b)−Ni(1)−N(1a)	98.47(8)
O(1a)−Ni(1)−O(3b)	87.06(7)	O(1b)−Ni(1)−O(3b)	85.22(7)
N(1b)−Ni(1)−O(3b)	88.33(8)	N(1a)−Ni(1)−O(3b)	172.37(8)
O(1a)−Ni(1)−O(3a)	85.37(7)	O(1b)−Ni(1)−O(3a)	87.58(7)
N(1b)−Ni(1)−O(3a)	172.23(8)	N(1a)−Ni(1)−O(3a)	87.58(7)
O(3b)−Ni(1)−O(3a)	84.81(8)		
Ni(2)−O(1c)	2.001(2)	Ni(2)−O(1c′)	2.001(2)
Ni(2)−N(1c)	2.074(2)	Ni(2)−N(1c′)	2.074(2)
Ni(2)−O(3c)	2.179(2)	Ni(2)−O(3c′)	2.179(2)
O(1c)−Ni(2)−N(1c)	88.71(9)	O(1c′)−Ni(2)−N(1c)	97.67(8)
O(1c)−Ni(2)−N(1c′)	97.67(8)	O(1c′)−Ni(2)−N(1c′)	88.71(9)
N(1c)−Ni(2)−N(1c′)	100.83(12)	O(1c)−Ni(2)−O(3c)	87.51(9)
O(1c′)−Ni(2)−O(3c)	84.97(9)	N(1c)−Ni(2)−O(3c)	170.34(9)
N(1c′)−Ni(2)−O(3c)	88.49(9)	O(1c)−Ni(2)−O(3c′)	84.97(9)
O(1c′)−Ni(2)−O(3c)	87.51(9)	N(1c)−Ni(2)−O(3c′)	88.49(9)
N(1c′)−Ni(2)−O(3c′)	170.34(9)	O(3c)−Ni(2)−O(3c′)	82.32(14)
O(1c)−Ni(2)−O(1c′)	170.01(12)		

Crystal Structure of 6

An ORTEP view of the copper complex **6** is shown in Figure 5. Complex **6** crystallizes in the monoclinic space group $P2_1/c$. The N atoms of the oxazoline five-membered ring and phenolato O atoms gave a distorted tetrahedral arrangement. Both tetrahedral and planar configurations have been reported for the related bis[*N*-alkylsalicylaldiminato(*O*−*N*)]copper(II) complexes, depending upon the nature of the alkyl groups.[22] For comparison with **6**, the complexes with α-branched *N*-alkyl groups should be considered. In the case of *i*Pr or *t*Bu groups, they were found to be pseudo-tetrahedral in the solid state. For example, bis[*N*-isopropylsalicylaldiminato(*O*−*N*)]copper(II) has a tetrahedral structure with an angle of 60° between the salicylaldiminato planes, whereas, *N*-Ph and *N*-Me substituted complexes are almost planar.[23,24] Lehn and co-workers have reported the crystal structure of a chiral bis(dihydrooxazole)copper(II) complex,[25] with a dihedral angle of 52° between the two N−Cu−N planes. Similar to the salicylaldiminato complexes, the oxazoline complexes also form both tetrahedral and square planar complexes depending upon the nature of the alkyl groups present on the five-membered ring. Bolm et al. have reported a Cu^{II} complex with a chiral oxazoline ligand in which the geometry around the metal center was found to be almost square planar.[6] However, the geometry around the metal center in complex **6** tends more towards tetrahedral which is probably due to the presence of the two methyl groups on the oxazoline ring. Bolm et al. have also reported that there is an interaction between the Cu atom of one molecule and the phenolate O atom of the neighboring molecule which make the Cu atoms pentacoordinate.[6] However, in complex **6** no such interactions were observed. In **6**, the angle between O(11)−Cu−N(1) and O(21)−Cu−N(2) planes is 30.8°, which indicates a distortion from planar geometry. The Cu−O distances [1.880(2) Å and 1.885(2) Å] and the Cu−N distances [1.985(2) Å, 1.986(2) Å] are similar to those reported for the chiral Cu^{II} complex[6] and bis(*N*-alkylsalicylaldiminato)copper(II) complexes.[24] In **6**, the angles of 91.76(7)° and 91.99(7)° for O(11)−Cu−N(1) and O(21)−Cu−N(2) are slightly smaller than the corresponding angles in bis(*N*-alkylsalicylaldiminato)copper(II) (94.4 and 95.0°). Significant bond lengths and angles for **6** are given in Table 3.

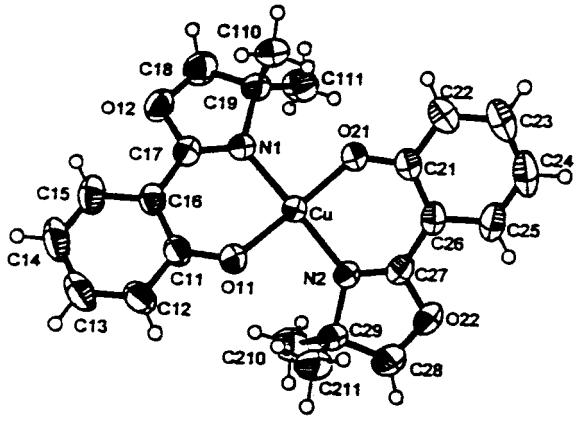

Figure 5. Crystal structure of complex **6**

Crystal Structure of 7

The colorless crystals of Zn^{II} complex **7** belong to the space group $P\bar{1}$ of the triclinic system. An ORTEP view of the structure is shown in Figure 6. Selected bond lengths and angles for **6** are given in Table 3. The Zn atom has a distorted tetrahedral coordination configuration. The interplanar angle between Zn−O(11)−N(1) and Zn−O(21)−N(2) is 86.2°. The planes between the phenyl ring and the heterocyclic ring are only slightly twisted. The dihedral angle between C(15)−C(16)−C(17)−O(12) is −0.9(3)°, that of C(15)−C(16)−C(17)−N(1) is −179.8(2)°. The Zn−O(11), Zn−O(21), Zn−N(1), and Zn−N(2) bond lengths are 1.9026(18), 1.9187(18), 1.9866(19), and 1.992(2) Å. Whereas the Zn−O distances do not differ substantially from values reported for similar Schiff base complexes,[26] the Zn−N distances are relatively short. However, the Zn−N bond lengths are slightly longer than the values reported for a similar oxazoline complex.[6]

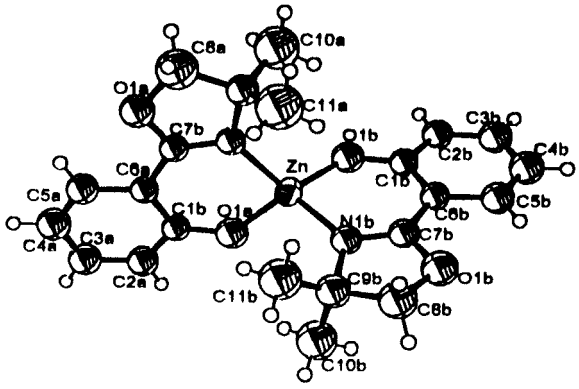

Figure 6. Crystal structure of complex **7**

Conclusion

In conclusion, we have shown that the 2-(4′,4′-dimethyl-3′,4′-dihydrooxazol-2′-yl)phenol ligand can be conveniently used to synthesize tetrahedral complexes of the late first row transition metals. Complexes **3**, **6**, and **7** crystallize as racemates in achiral space group, however, for complex **7**, the interconversion between the (*M*) and (*P*) helix is slow at low temperatures. Since the other complexes (Co, Ni, Cu) are found to be paramagnetic, the variable-temperature NMR spectroscopy of these complexes, which is used to study their low-temperature behavior, could not be attempted. The solid-state structures show that none of these complexes are chiral. Similar to the behavior of Agrobactin, the ligand 2-(4′,4′-dimethyl-3′,4′-dihydrooxazol-2′-yl)-phenol undergoes metal-assisted hydrolysis/oxidation in the presence of oxophilic Mn^{III} ions to give the partially hydrolyzed oxazoline ring as found in Agrobactin A, forming a novel mononuclear complex. The ability of Ni^{II} to form six-coordinate complexes with neutral ligands allows the

isolation of a novel octahedral Ni^{II} complex with a neutral acetic acid ligand.

Experimental Section

General Procedures: Solvents were purified by standard procedures[27] and were freshly distilled prior to use. 2-Amino-1-methyl-1-propanol (Merck) and $ZnCl_2$ were also purified prior to use.[27] 2-Hydroxybenzonitrile (Merck) was used as received. − Melting points were recorded in capillary tubes and are uncorrected. − IR spectra were recorded as KBr pellets with a Nicolet Impact 400 FT-IR spectrometer. − For **1** and **7**, the ^1H, and ^{13}C spectra were obtained at 300 and 75.42 MHz in $CDCl_3$ with a Varian VXR 300S spectrometer. Chemical shifts are cited with respect to $SiMe_4$ as an internal standard. − Elemental analyses were performed with a Carlo−Erba model 1106 elemental analyzer. − Fast atom bombardment (FAB) mass spectra were recorded at room temperature with a JEOL SX 102 DA-6000 mass spectrometer/data system using xenon (6 kV, 10 mV) as the bombarding gas. − Cyclic Voltammetry (CV) experiments were performed with an EPΣG Princeton Applied Research Potentiostat/Galvanostat Model 273A which consisted of a one-compartment cell with platinum working and counter electrodes and an Ag−AgCl electrode (reference electrode). Tetraethylammonium perchlorate was used as the supporting electrolyte. All solutions were purged with argon or nitrogen and retained under these gases while the CV data were recorded. − The EPR spectra of the complexes in chloroform or ethanol were recorded with a Varian E-112 EPR spectrometer using tetracyanoethylene as *g* marker ($g = 2.00277$) at room temperature and liquid-nitrogen temperatures. − Magnetic susceptibilities of powdered samples were determined at room temperature with a Faraday balance, standardized with mercury tetracyanocobaltate(II) [$\chi = 16.44 \cdot 10^{-6}$ cm^3 mol^{-1}]. The molar susceptibilities were corrected for ligand diamagnetism using Pascal's constants. The effective magnetic moments were calculated using the expression $\mu_{eff} = 2.83(\chi_m \times T)^{1/2}$. − Electronic absorption spectra were obtained in $CHCl_3$ at 25 °C in a 1-cm quartz cuvette with a Shimadzu UV-2100 apparatus.

Synthesis of 2-(4′,4′-Dimethyl-3′,4′-dihydrooxazol-2′-yl)phenol (1): This compound was synthesized by following the published procedure with minor modifications.[5] 2-Amino-1-methyl-1-propanol (5.99 g, 6.41 mL, 67.20 mmol), 2-hydroxybenzonitrile (5.35 g, 44.91 mmol), and $ZnCl_2$ (0.31 g, 2.24 mmol) were dissolved in chlorobenzene (90 mL) and refluxed for 24 h under nitrogen. The resulting reaction mixture was filtered to remove the undissolved impurities. The filtrate was concentrated under reduced pressure to give a brown oil which was dissolved in 50 mL of CH_2Cl_2 and washed with water. The organic layer was separated, dried with anhydrous Na_2SO_4, filtered, and concentrated to give the desired compound as a light brown oil.

Synthesis of [Mn(OR){O(Ox)}$_2$] (2): To a solution of $Mn(OAc)_2 \cdot 4\,H_2O$ (0.25 g, 1.02 mmol) in absolute ethanol (20 mL) was added a solution of **1** (0.38 g, 1.99 mmol) in ethanol (10 mL). The reaction mixture was stirred for 24 h at room temperature. The resulting dark green solution was concentrated under reduced pressure to give a dark oil. This was dissolved in dry ether (20 mL) and filtered through Celite to remove the undissolved impurities. Addition of hexane (20 mL) to the ethereal solution followed by cooling of the solution overnight afforded a black-green solid. The solid was filtered off, washed with hexane and dried under reduced pressure to give **2** as a black-green crystalline solid. Compound **2** was recrystallized by slow concentration of a solution of **2** in 1:1 mixture of CH_2Cl_2 (5 mL)/CH_3OH (5 mL) at room temperature to give black-green crystals. Yield: 0.31 g (48%). − M.p. 180−182°C. − $C_{33}H_{38}MnN_3O_7$ (643.6): calcd. C 61.58, H 5.95, N 6.53; found C 61.52, H 5.10, N 6.13. − MS; *m/z*: 453 $[C_{22}H_{26}N_2O_5Mn]^+$, 435 $[C_{22}H_{24}N_2O_4Mn]^+$, 293 $[C_{11}H_{14}NO_5Mn]^+$, 244 $[C_{11}H_{12}NO_2Mn]^+$, 191 $[C_{11}H_{12}NO_2]^+$, 173 $[C_{11}H_{12}NO]^+$. − IR (KBr): $\tilde{\nu}$ = 1580 cm^{-1}(C=O), 1609 cm^{-1}(C=N). − EPR (Solid & $CDCl_3$, 298 K): Silent.

Synthesis of [Co{O(Ox)}$_2$] (3): To a solution of $Co(OAc)_2 \cdot 4\,H_2O$ (0.25 g, 1.01 mmol) in absolute ethanol (20 mL) was added a solution of **1** (0.38 g, 1.99 mmol) in ethanol (10 mL). A pink-colored compound precipitated immediately. The stirring was continued for 12 h at room temperature. The resulting crude solid was filtered and dried under vacuum. Pink-colored needle-shaped crystals of the desired compound **3** were obtained by slow concentration of a CH_2Cl_2(5 mL)/methanol(5 mL) solution of the crude product at room temperature. Yield: 0.37g (85%). − M.p. 234−236°C. − $C_{22}H_{24}CoN_2O_4$ (439.4): calcd. C 60.14, H 5.50, N 6.38; found C 60.23, H 5.35, N 6.22. − MS; *m/z* (%): 439 $[M^+, C_{22}H_{24}N_2O_4Co]^+$ (100), 364 $[C_{22}H_{24}N_2O_3]^+$, 249 $[C_{11}H_{12}NO_2Co]^+$, 190 $[C_{11}H_{12}NO_2]^+$, 177 $[C_{11}H_{12}NO]^+$. − IR (KBr): $\tilde{\nu}$, 1618 cm^{-1} (C=N).

Synthesis of [Ni{O(Ox)}$_2$] (4): To a solution of $Ni(OAc)_2 \cdot 4\,H_2O$ (0.25 g, 1.01 mmol) in absolute ethanol (20 mL) was added a solution of **1** (0.38 g, 1.99 mmol) in ethanol (10 mL). The resulting green solution was stirred for 18 h at room temperature. The pale green solid formed was filtered and washed with ethanol and dried under vacuum. The pale green crystals of **4** were obtained by slow concentration of a CH_2Cl_2(5 mL)/ethanol(5 mL) solution of the crude product. Slow concentration of the filtrate at room temperature afforded the dark green crystals of **5**.

4: Yield: 0.26g (60%). − M.p. 224−226°C. − $C_{22}H_{24}N_2NiO_4$ (439.2): calcd. C 60.17, H 5.51, N 6.38; found C 59.84, H 5.32, N 6.10. − MS; *m/z* (%): 555 $[C_{26}H_{32}N_2O_8Ni]^+$, 496 $[C_{24}H_{28}N_2O_6Ni]^+$, 439 $[C_{22}H_{24}N_2O_4Ni]^+$, 424 $[C_{21}H_{21}N_2O_4Ni]^+$, 367 $[C_{15}H_{20}NO_6Ni]^+$, 352 $[C_{14}H_{17}NO_6Ni]^+$, 248 $[C_{11}H_{12}NO_2Ni]^+$, 176 $[C_{11}H_{12}NO]^+$ (100). − IR (KBr): $\tilde{\nu}$ = 1622 cm^{-1} (C=N). − EPR (Solid, 77 K): $g_{eff} = 2.18$.

5: Yield: 0.17g (30%). − M.p. 198−200°C. − $C_{26}H_{32}N_2NiO_8$ (559.3): calcd. C 55.84, H 5.77, N 5.01; found C 55.54, H 5.45, N 4.87. − MS; *m/z* (%): 555 [M, $C_{26}H_{32}N_2O_8Ni]^+$ (100), 498 $[C_{24}H_{28}N_2O_6Ni]^+$, 439 $[C_{22}H_{24}N_2O_4Ni]^+$, 424 $[C_{21}H_{21}N_2O_4Ni]^+$, 365 $[C_{15}H_{20}NO_6Ni]^+$, 352 $[C_{14}H_{17}NO_6Ni]^+$, 248 $[C_{11}H_{12}NO_2Ni]^+$, 176 $[C_{11}H_{12}NO]^+$. − IR (KBr): $\tilde{\nu}$ = 1617 cm^{-1} (C=N), 1706 cm^{-1} (C=O). − EPR (Solid & $CDCl_3$, 298 K): Silent.

Synthesis of [Cu{O(Ox)}$_2$] (6): To a solution of $Cu(OAc)_2 \cdot H_2O$ (0.20 g, 1.01 mmol) in absolute ethanol (20 mL) was added a solution of **1** (0.38 g, 1.99 mmol) in ethanol (10 mL). The resulting green-colored solution was stirred for 24 h at room temperature and then filtered. The filtrate was concentrated under vacuum to give a green-colored solid. Recrystallization of the solid from CH_2Cl_2(5 mL)/methanol(5 mL) mixture at room temperature afforded the dark green crystals of **6**. Yield: 0.38g (85%). − M.p. 190−192°C. − $C_{22}H_{24}CuN_2O_4$ (443.10): calcd. C 59.52, H 5.45, N 6.31; found C 59.27, H 5.23, N 6.14. − MS; *m/z* (%): 443 [M, $C_{22}H_{24}N_2O_4Cu]^+$ (100), 371 $[C_{22}H_{24}N_2O_3]^+$, 253 $[C_{11}H_{12}NO_2Cu]^+$, 191 $[C_{11}H_{12}NO_2]^+$, 176 $[C_{11}H_{12}NO]^+$. − IR(KBr): $\tilde{\nu}$ = 1614 cm^{-1} (C=N). − EPR ($CHCl_3$, 25 °C): g_{eff} = 2.31.

Synthesis of [Zn{O(Ox)}$_2$] (7): To a solution of $Zn(OAc)_2$ (0.46 g, 2.51 mmol) in absolute ethanol (30 mL) was added a solution of **1** (0.95 g, 4.97 mmol) in ethanol (10 mL). The reaction mixture was stirred for 24 h at room temperature during which time a white solid was formed. The solid was filtered and dried under vacuum. Colorless crystals of the desired compound were obtained by recrystallization from $CHCl_3$(5 mL)/hexane (5 mL). Yield: 0.40 g (90%). − M.p. 210−212 °C. − $C_{22}H_{24}N_2O_4Zn$ (445.8): calcd. C 59.27, H 5.43, N 6.28; found C 59.14, H 5.22, N 6.16. − ^{1}H NMR ($CDCl_3$): δ = 1.38 (s, 12 H, CH_3), 4.16(s, 4 H, CH_2), 6.52−6.56 (dd, 2 H, Ar-H), 6.84−6.88 (d, 2 H, Ar-H) 7.25−7.33 (dd, 2 H, Ar-H), 7.67−7.71 (d, 2 H, Ar-H). − ^{13}C NMR ($CDCl_3$): δ = 28.34, 66.39, 77.77, 108.95, 113.86, 123.14, 130.05, 134.99, 168.11, 170.27. − MS; *m/z* (%): 702 $[C_{33}H_{36}N_3O_6Zn_2]^+$, 445 [M, $C_{22}H_{24}N_2O_4Zn]^+$ (100), 254 $[C_{11}H_{12}NO_2Zn]^+$, 238 $[C_{10}H_9NO_2Zn]^+$, 191 $[C_{11}H_{12}NO_2]^+$. − IR (KBr): $\tilde{\nu}$ = 1645 cm^{-1} (C=N).

X-ray Crystallographic Studies: The diffraction measurements for compounds **2**, **3**, **5**, **6**, and **7** were performed at room temperature (293 K) with a Siemens R3m/V diffractometer using graphite-monochromated Mo-K_α radiation (λ = 0.71073 Å). The unit cell was determined from 25 randomly selected reflections using the automatic search index and least-squares routine. For **2**, the θ range for data collection was from 2.25 to 27.50° whereas for **3**, **5**, **6**, and **7** the ranges were 2.58−27.50°, 1.29−27.50°, 2.40−27.50°, and 2.58−50.59°. The index range for **2** was $-13 \le h \le 0$, $-13 \le k \le 13$, $-19 \le l \le 20$ while for **3**, **5**, **6**, and **7** the ranges were $0 \le h \le 10$, $-13 \le k \le 13$, $-16 \le l \le 17$; $0 \le h \le 41$, $-20 \le k \le 0$, $-21 \le l \le 21$; $-14 \le h \le 0$, $0 \le k \le 12$, $-25 \le l \le 25$, and $0 \le h \le 11$, $-14 \le k \le 14$, $-18 \le l \le 18$. The data for **3**, **6**, and **7** were corrected for Lorentz, polarization, and absorption effects. The maximum and minimum transmission values of the correction factors for compounds **3** (dimensions 0.48 × 0.50 × 0.49 mm), **6** (0.19 × 0.88 × 0.38 mm), and **7** (0.28 × 0.64 × 0.32 mm) were 0.4733 and 0.3904, 0.2873 and 0.2187, and 0.9181 and 0.8319. The data were monitored by measuring two standard reflections every 60 min of X-ray exposure time. The structures were solved by routine heavy-atom (using SHELXS 86[28]) and Fourier methods and refined by full-matrix least squares with the non-hydrogen atoms anisotropic and hydrogen atoms with fixed isotropic thermal parameters of 0.07 Å^2 using the SHELXL 93 program.[29] The hydrogen atoms were partially located from difference electron-density maps and the rest were fixed at calculated positions. Scattering factors were from common sources.[30] Some details of data collection and refinement are given in Table 5 and Table 6. Crystallographic data (excluding structure factors) for the structures reported in this paper have been deposited with the Cambridge Crystallographic Data Centre as supplementary publications nos. CCDC-134052 (**2**), -134053 (**3**), -134054 (**5**), -134055 (**6**), -134056 (**7**). Copies of the data can be obtained free of charge on application to CCDC, 12 Union Road, Cambridge CB21EZ, UK [Fax: (internat.) + 44-1223/336-033; E-mail: deposit@ccdc.cam.ac.uk].

Table 6. Crystal data and structure refinement for **6** and **7**

	6	**7**
Empirical formula	$C_{22}H_{24}CuN_2O_4$	$C_{22}H_{24}N_2O_4Zn$
Molecular mass	443.97	445.80
Crystal system	monoclinic	triclinic
Space group	$P2_1/c$	$P\bar{1}$
a [Å]	11.462(2)	8.0231(8)
b [Å]	9.3919(12)	11.4838(13)
c [Å]	19.628(2)	13.2563(13)
α [°]	90	115.582(7)
β [°]	91.726(8)	96.924(6)
γ [°]	90	94.500(7)
V [Å^3]	2112.0(4)	1081.9(2)
Z	4	2
D(calcd.) [Mg/m^3]	1.396	1.368
Abs. coeff. [mm^{-1}]	1.064	1.164
Obsd. reflexions [$I > 2\sigma$]	4800	5969
Final $R(F)$ [$I > 2\sigma(I)$][a]	0.0358	0.0432
$wR(F^2)$ indices [$I > 2\sigma(I)$]	0.0928	0.1132
Data/restrains/parameters	4799/0/291	5968/0/291
Goodness of fit on F^2	1.03	1.07

[a] Definitions: $R(F_o) = ||F_o| - |F_c||/|F_o|$ and $wR(F_o^2) = \{[w(F_o^2 - F_c^2)^2]/[w(F_c^2)^2]\}^{1/2}$.

Acknowledgments

We are grateful to the Department of Science and Technology (DST), New Delhi and Board of Research in Nuclear Sciences (BRNS), Department of Atomic Energy, Bombay for funding this work. Additional help from the Regional Sophisticated Instrumentation Centre (RSIC), Indian Institute of Technology (IIT),

Table 5. Crystal data and structure refinement for **2**, **3**, and **5**

	2	**3**	**5**
Empirical formula	$C_{33}H_{38}N_3O_7Mn$	$C_{22}H_{24}N_2O_4Co$	$C_{26}H_{32}N_2O_8Ni$
Molecular mass	643.60	439.36	559.25
Crystal system	triclinic	triclinic	monoclinic
Space group	$P\bar{1}$	$P\bar{1}$	$C2/c$
a [Å]	10.095(2)	8.018(2)	31.690(6)
b [Å]	10.646(2)	11.472(3)	15.401(2)
c [Å]	15.734(4)	13.230(3)	16.856(3)
α [°]	94.76(2)	64.581(14	90
β [°]	108.22(2)	79.358(14)	97.083(9)
γ [°]	91.14(2)	85.54(2)	90
V [Å^3]	1598.7(6)	1080.2(5)	8164(2)
Z	2	2	12
D(calcd.) [Mg/m^3]	1.337	1.351	1.365
Abs. coeff. [mm^{-1}]	0.464	0.823	0.763
Obsd. reflexions [$I > 2\sigma$]	7332	4345	9231
Final $R(F)$ [$I > 2\sigma(I)$][a]	0.0558	0.0344	0.0427
$wR(F^2)$ indices [$I > 2\sigma(I)$]	0.1267	0.0917	0.1019
Data/restrains/parameters	7328/0/447	4345/0/291	9228/0/567
Goodness of fit on F^2	1.043	1.09	1.08

[a] Definitions: $R(F_o) = ||F_o| - |F_c||/|F_o|$ and $wR(F_o^2) = \{[w(F_o^2 - F_c^2)^2]/[w(F_c^2)^2]\}^{1/2}$.

Bombay, for EPR and 300-MHz NMR spectroscopy is gratefully acknowledged. R. J. B. wishes to acknowledge the DoD-ONR program for funds to upgrade the diffractometer.

[1] [1a] S. A. Ong, T. Peters, J. B. Neilands, *J. Biol. Chem.* **1979**, *254*, 1860. – [1b] T. Peterson, J. B. Neilands, *Tetrahedron Lett.* **1979**, *50*, 4805. – [1c] T. Peterson, K. -E. Falk, S. A. Leong, M. P. Klein, J. B. Neilands, *J. Am. Chem. Soc.* **1980**, *102*, 7715. – [1d] Y. Nagao, T. Miyasaka, Y. Hagiwara, E. Fujita, *J. Chem. Soc., Perkin Trans. 1* **1984**, 183. – [1e] D. L. Eng-Wilmot, D. van der Helm, *J. Am. Chem. Soc.* **1980**, *102*, 7719.

[2] A. Jacobs, G. P. White, G. H. Tait, *Biochem. Biophys. Res. Commun.* **1977**, *74*, 1626.

[3] [3a] H. Brunner, H. Nishiyama, K. Itoh, in: *Catalytic Asymmetric Synthesis* (Ed.: I. Ojima), VCH Publishers, New York, **1993**, p. 303. – [3b] J. V. Allen, J. M. J. Williams, *Tetrahedron: Asymmetry* **1994**, *5*, 277. – [3c] H. Brunner, D. Henrichs, *Tetrahedron: Asymmetry* **1995**, *6*, 653. – [3d] E. Macedo, C. Moberg, *Tetrahedron: Asymmetry* **1995**, *6*, 549. – [3e] H. Eichelmann, H.-J. Gais, *Tetrahedron: Asymmetry* **1995**, *6*, 643. – [3f] C. J. Richards, D. E. Hibbs, M. B. Hursthouse, *Tetrahedron Lett.* **1995**, *36*, 3745.

[4] [4a] P. G. Cozzi, C. Floriani, A. C. Villa, C. Rizzoli, *Inorg. Chem.* **1995**, *34*, 2921. – [4b] P. G. Cozzi, C. Floriani, *J. Chem. Soc., Perkin Trans.1* **1995**, 2557.

[5] [5a] M. G. Simon, S. Jansat, G. Muller, D. Panyella, M. F. Bardia, X. Soians, *J. Chem. Soc., Dalton Trans.* **1997**, 3755. – [5b] M. Hoogenraad, K. Ramkisoensing, H. Kooijman, A. L. Spek, E. Bouwman, J. G. Haasnoot, J. Reedijk, *Inorg. Chim. Acta* **1998**, *279*, 217.

[6] H. R. Hoveyda, V. Karunaratne, S. J. Rettig, C. Orvig, *Inorg. Chem.* **1992**, *31*, 5408.

[7] C. Bolm, K. Wieghardt, M. Zehnder, D. Glasmacher, *Helv. Chim. Acta* **1991**, *74*, 717.

[8] C. Bolm, K. Wieghardt, M. Zehnder, T. Renff, *Chem. Ber.* **1991**, *124*, 1173.

[9] [9a] H. B. Singh, N. Sudha, *Coord. Chem. Rev.* **1994**, *135–136*, 469. – [9b] R. Kaur, H. B. Singh, R. J. Butcher, *Organometallics* **1995**, *14*, 4755. – [9c] R. Kaur, H. B. Singh. R. P. Patel, S. K. Kulshreshtha, *J. Chem. Soc., Dalton Trans.* **1996**, 461. – [9d] S. C. Menon, H. B. Singh, J. M. Jasinski, J. P. Jasinski, R. J. Butcher, *Organometallics* **1996**, *15*, 1707. – [9e] S. C. Menon, H. B. Singh, R. P. Patel, K. Das, R. J. Butcher, *Organometallics* **1997**, *18*, 563. – [9f] G. Mugesh, A. Panda, H. B. Singh, N. S. Punekar R. J. Butcher, *Chem. Commun.* **1998**, 2227. – [9g] G. Mugesh, H. B. Singh, R. J. Butcher, *Tetrahedron: Asymmetry* **1999**, *10*, 237. – [9h] G. Mugesh, A. Panda, H. B. Singh, R. J. Butcher, *Chem. Eur J.* **1999**, *5*, 1411. – [9i] A. Panda, G. Mugesh, H. B. Singh, R. J. Butcher, *Organometallics* **1999**, *18*, 1986.

[10] [10a] G. Mugesh, H. B. Singh, R. J. Butcher, *Eur. J. Inorg. Chem.* **1999**, 1229. – [10b] G. Mugesh, H. B. Singh, R. P. Patel, R. J. Butcher, *Inorg. Chem.* **1998**, *37*, 2663. – [10c] G. Mugesh, H. B. Singh, R. J. Butcher, *J. Organomet. Chem.* **1999**, *577*, 243.

[11] [11a] M. Schroder, "Nickel: Inorganic and Coordination Chemistry" in: *Encyclopedia of Inorganic Chemistry* (Ed.: R. B. King) John Wiley & Sons, New York, **1994**, vol. 4, p. 2392. – [11b] D. Volkmer, A. Horstmann, K. Griesar, W. Haase, B. Krebs, *Inorg. Chem.* **1996**, *35*, 1132.

[12] B. N. Figgis, *Nature* **1958**, *182*, 1568.

[13] R. L. Carlin Jr., S. L. Holt, *Inorg. Chem.* **1963**, *2*, 849.

[14] F. A. Cotton, D. M. L. Goodgame, M. Goodgame, *J. Am. Chem. Soc.* **1961**, *83*, 4690.

[15] H. Yokoi, T. Isobe, *Bull. Chem. Soc. Jpn.* **1969**, *42*, 2187.

[16] B. P. Kennedy, A. B. P. Lever, *J. Am. Chem. Soc.* **1973**, *95*, 6907.

[17] V. M. Miskowski, J. A. Thich, R. Solomon, H. J. Schugar, *J. Am. Chem. Soc.* **1976**, *98*, 8344.

[18] A. R. Amundsen, J. Whelan, G. Bosnich, *J. Am. Chem. Soc.* **1977**, *99*, 6730.

[19] G. Das, R. Shukla, S. Mandal, R. Singh, P. K. Bharadwaj, J. Van Hall, K. H. Whitmire, *Inorg. Chem.* **1997**, *36*, 323.

[20] W. D. Horrocks, J. N. Ishley, R. R. Whittle, *Inorg. Chem.* **1982**, *21*, 3265.

[21] W. D. Horrocks, J. N. Ishley, R. R. Whittle, *Inorg. Chem.* **1982**, *21*, 3270.

[22] P. L. Orioli, L. Sacconi, *J. Am. Chem. Soc.* **1966**, *88*, 277.

[23] E. C. Lingafelter, G. L. Simmons, B. Morosin, C. Scheringer, C. Freiburg, *Acta Crystallogr.* **1961**, *14*, 1222.

[24] L. Wei, R. M. Stogsdill, E. C. Lingafelter, *Acta Crystallogr.* **1964**, *17*, 1058.

[25] J. Hall, J. -M. Lehn, A. DeCian, J. Fisher, *Helv. Chim. Acta* **1991**, *74*, 1.

[26] R. H. Prince, in: *Comprehensive Coordination Chemistry* (Eds.: G. Wilkinson, R. D. Gilliard, J. A. McCleverty), Pergamon Press, Oxford, **1987**, vol. 5, pp. 925.

[27] D. D. Perrin, W. L. F. Armarego, D. R. Perrin, *Purification of Laboratory Chemicals*, 2nd ed., Pergamon, Oxford, **1980**.

[28] G. M. Sheldrick, *Crystallographic Computing 3*, Oxford University Press, Oxford, **1985**, p. 175.

[29] G. M. Sheldrick, *SHELX 93, Program for Crystal Structure Determination*, University of Göttingen, **1993**.

[30] *International Tables for X-ray Crystallography*, Kynoch Press, Birmingham, **1974**, vol. 4, pp. 99, 149.

Received June 30, 2000
[I00259]